Expert-Rule-Based Gain Adjustment for PID and Fuzzy Controllers under Step and Continuous Inputs

Phichitphon Chitikunnan ¹, Panya Minyong ²,*, Nuntachai Thongpance ¹, Rawiphon Chotikunnan ¹, Anuchit Nirapai ¹, Pariwat Imura ¹, Wanida Khotakham ¹, Kittipan Roongprasert ¹, and Anantasak Wongkamhang ¹,*

¹College of Biomedical Engineering, Rangsit University, Pathum Thani, Thailand

² Mechatronics and Robotics Engineering established under the Faculty of Technical Education,
Rajamangala University of Technology Thanyaburi, Pathum Thani, Thailand
Email: phichitphon.c@rsu.ac.th (P.C.); panya_m@rmutt.ac.th (P.M.); nuntachai.t@rsu.ac.th (N.T.);
rawiphon.c@rsu.ac.th (R.C.); anuchit.ni@rsu.ac.th (A.N.); pariwat.i@rsu.ac.th (P.I.); wanida.k@rsu.ac.th (W.K.);
kittipan.r@rsu.ac.th (K.R.); anantasak.w@rsu.ac.th (A.W.)

*Corresponding author

Abstract—This investigation introduces a novel dual-expert gain scheduling framework for robotic manipulators that is intended to accommodate both abrupt step inputs and steady trajectories in simulation conditions. There are two adaptive controllers that are proposed: the Fuzzy Logic-based Dual Expert Controller (FBDEC) and the Proportional Integral Derivative-based Dual Expert Controller (PBDEC). Each utilizes a classification mechanism that is expert-based in order to dynamically alternate between step and smooth specific gain criteria. PBDEC reduces overshoot to below 9% and obtains up to 47% lower Integral Absolute Error (IAE) and Root Mean Square Error (RMSE) compared to classical Proportional-Integral-Derivative (PID), as evidenced by simulation results on a three-jointed robotic platform. Similarly, FBDEC surpasses conventional fuzzy control by enhancing tracking precision and restricting overshoot to less than 3%. The dual-expert approach, in contrast to traditional single-mode systems, provides a high level of accuracy and a rapid response, seamlessly adapting to a variety of reference profiles. This study delivers the first systematic performance benchmark of PID and fuzzy logic controllers integrated with dual-expert systems across step and smooth inputs, thereby confirming their superiority in terms of generalizability, tracking, and resilience.

Keywords—adaptive control, dual expert control, expert-based gain adjustment, fuzzy logic controller, Proportional-Integral-Derivative (PID) controller, gain scheduling, trajectory classification, robotic manipulator, step input rejection, online rule switching

I. INTRODUCTION

Industrial robotic manipulators are instrumental in the advancement of modern manufacturing, medical intervention, and service automation, as they offer high throughput and micrometer-level accuracy. Despite these capabilities, adaptability is constrained by two persistent

control issues. The reference profile has a substantial impact on the controller's efficacy at the outset. The reverse is also true; loops that are optimized for abrupt step commands frequently exhibit poor tracking of smooth trajectories [1–4]. Secondly, the accumulation of minor modelling errors and cycle-to-cycle disturbances over protracted periods results in fluctuations in position or force

As a result, the Proportional-Integral-Derivative (PID) control has experienced a swift transformation. Fuzzy-PID hybrids [1] are used to smooth brushless-Direct Current (DC) responses, including variable-structure designs for electric-vehicle motors [5]. Practical DC-motor platforms, such as classical PID implementations and fuzzy self-tuning variants, have demonstrated overshoot and settling-time benefits in hardware-in-the-loop studies and simulations [6, 7]. The robustness of fractional-order PID is improved by bee colony optimization [3], and evolutionary search generates gains that are nearly optimal for micro-robots [1]. Parallel work in Fuzzy-Logic Control (FLC) has reported successful gain scheduling for mobile-robot tracking and lower steady-state errors than classical PI in permanent-magnet synchronous motors [8, 9]. Beyond robotics, fuzzy PID has been used to improve power-system stability and constrained-orbit transfer under uncertainty [10, 11].

A recurring limitation is that the overwhelming majority of PID, FLC, and hybrid approaches are single-mode. Gains are predetermined offline for a single reference type, and any modification to the profile requires retuning. Existing profile-aware methods, including type-2 fuzzy loops or Particle Swarm Optimization—Proportional Derivative (PSO-PD) schemes, continue to assume constant inputs after deployment [12–16]. Adaptive fuzzy logic has also been examined in practice-oriented robotics

Manuscript received June 23, 2025; revised July 7, 2025; accepted August 8, 2025; published November 11, 2025.

594

for electro-hydraulic actuators and multi-rotor vehicles; however, these controllers typically remain tied to a single operating profile once tuned [17, 18]. The present work addresses this limitation by introducing an expert-rule gain-scheduling approach that instantly loads the corresponding gains. In this approach, each reference sample is classified as either "step" or "smooth". Two controllers are under investigation: Proportional Integral Derivative-based Dual Expert Controller (PBDEC) (PID-based) and Fuzzy Logic-based Dual Expert Controller (FBDEC) (fuzzy-PD-based). Both are evaluated against classical PID, standard FLC, and four single-expert baselines in a simulated environment of the three-axis Seiko D-Tran RT3200 robot. The results suggest that PBDEC can reduce Integral Absolute Error (IAE) and Root-Mean-Square Error (RMSE) by up to 46.9% while limiting overshoot to 9%, and FBDEC can reduce overshoot to below 3% during ramp tracking. Consequently, dual-expert scheduling offers a flexible and consistent solution that is suitable for a diverse array of applications, such as precision assembly and medical robotics.

II. LITERATURE REVIEW

A. PID and Optimisation-Enhanced PID

The primary emphasis of early PID research was conventional tuning; however, more recent research has prioritized intelligent optimization. Fuzzy-PID combinations improve the smoothness of Brushless Direct Current (BLDC) motor responses bee-colony [3], genetic-algorithm [19–21], and particle swarm optimization methods [22, 23] automate gain selection. The robustness of fractional-order PIDs is enhanced by bee-colony search [3], and the stability of hybrid power systems is improved by hybrid GWO-fuzzy or Grey-Wolf designs [24]. The practical DC-motor case studies [6, 7] document baseline PID design and as well as fuzzy self-tuning implementation, enhancements. Several surveys summarize the capabilities and limitations of these modern techniques [3, 4].

B. Fuzzy-Logic Control (FLC) and Hybrids

Takagi-Sugeno loops outperform PI on PMSM drives [8]. Fuzzy logic controller-based Battery Energy Storage System (BESS) regulators stabilize pico-hydro plants [25], whereas Programmable Logic Controller (PLC)-integrated fuzzy logic controllers regulate conveyor positioning [26]. Hybrid fuzzy-PID loops are utilized to direct quadcopters [27]. The trajectories electro-hydraulic actuators and quadrotors were tracked using hybrid robust fuzzy-PID with disturbance accommodation [17, 18]. Fuzzy control has also been employed in water-jet devices [28]. The hardware feasibility of Arduino-based sliding-mode control is confirmed [29], and the settling times of servo drives are reduced by fuzzy self-tuning [30]. Grey-Wolf-optimized fuzzy-PID reduces hybrid-grid frequency deviations [24], while pure FLC maintains BLDC speed in the presence of load fluctuations [31]. Object-sorting tasks using 4-DOF manipulators have also been controlled through fuzzy logic [32], and membership-function tuning for manipulator control has been systematically optimized [33].

C. Advanced FLC Applications in Robotics

Multi-level fuzzy inference improves the accuracy of unmanned-vehicle hand-off decisions [34]. Pure FLC is capable of navigating dense storage containers [35]. The adaptive fuzzy dynamic-surface control reduces the complexity of Mecanum wheels [36]. Fuzzy planners decrease warehouse travel time [37, 38]. Vibrations in confined passages are mitigated by fuzzy sliding-mode Fuzzy Linear Quadratic Regulator Proportional Integral Derivative (Fuzzy-LOR-PID) and fuzzy-PID fractional-order improve immunity [40, 41]. The avoidance of obstacles is facilitated by fuzzy control [42], quadcopter gain self-tuning [43], and Robot Operating System (ROS)-based feedback linearization [44]. Adaptive fuzzy manipulation, repetitive control, and dual-design iterative learning are all effective methods for enhancing precision-arm performance [45–52].

D. Broader Rule-Based Control Domains

Proportional-Integral-Derivative (PID) and fuzzy variants are employed in a diverse array of applications, such as the regulation of renewable energy [53–56], the pasteurization of milk [57], the detection of wireless sensor anomalies [58–60], the diagnostics of rotating machines [61], the enhancement of underwater video [62], the enhancement of underwater video [63], the coordination of Mivar-based robots [64], and the development of extensive fuzzy expert system surveys [59, 65]. Offshore-platform safety scoring [66] and medical diagnosis algorithms [67] extend rule-based control beyond robotics.

E. Profile-Specific Research and Existing Gaps

The fuzzy-membership morphologies of manipulators that executed both step and smooth profiles were contrasted in a recent study. The investigation determined that triangular sets were more effective for step inputs, while bell sets provided higher precision for smooth trajectories [68]. In addition, the control of PD in Delta and Par4 mechanisms has been examined profile-specific tailoring for Cartesian adaptation in R4 limbs [12] and PSO-augmented mechanisms [13]. Adaptive gain scheduling was found to be rarely implemented according to a survey of parallel-robot control conducted from 2008 to 2024 [14]. Type-2 fuzzy controllers [16] are single-mode and lack the capacity to modify profiles in real time, despite their advantages. Fault detection schemes [15], while intelligent, are not designed accommodate profile variation. manipulator-focused research on membership-function tuning has introduced data-driven procedures; however, a fixed operating profile is still presumed after the tuning process is complete [33]. Consequently, the current PID, FLC, and hybrid controllers rely on offline gains to produce a unique reference profile. PSO-PD schemes are unable to transition online [13], and type-2 fuzzy loops typically assume static inputs [16].

III. ROBOTIC MANIPULATORS AND SYSTEM MODELING FOR APPLICATIONS

This section provides a comprehensive description of the Seiko D-Tran RT3200 robotic manipulator, which is classified as a cylindrical-type robot. This robot is particularly well-suited for machine tending and material handling tasks in constrained environments because of its capacity to perform vertical and radial movements within a compact footprint. It also addresses the development of mathematical models for the system, the design of control methods such as PID and fuzzy logic controllers, and the construction of a smart control system capable of autonomously adjusting gain values. The selection of appropriate controller gains will also be discussed in the subsequent sections, taking into account the characteristics of the input signals.

A. Design and Implementation of the Seiko D-Tran RT3200 Robotic Structure

The Seiko D-Tran RT3200 is an autonomous manipulator of the cylindrical type. It is equipped with four joints: T and A for rotation in the X-Y plane, R for translation along the X-axis, and Z for vertical motion. It is designed for industrial and research environments that necessitate precise operations. In order to guarantee synchronized and stable actuator coordination, a National Instruments cRIO-9075 controller is utilized to connect a LabVIEW interface to four motor drivers, as illustrated in Fig. 1. Subsequently, real-time control and monitoring are implemented.

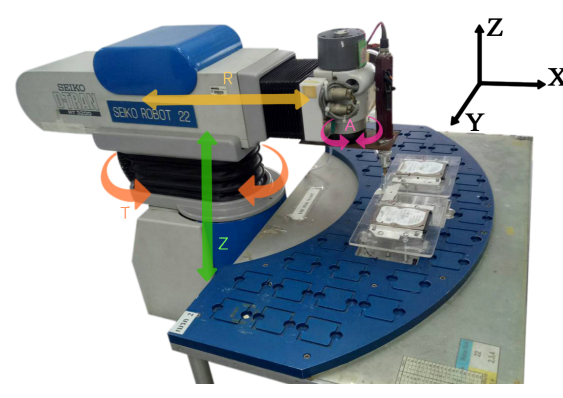


Fig. 1. Seiko D-Tran RT3200.

The system operates in a discrete-time model with a fixed sampling interval of 0.055 s. Closed-loop experiments were implemented to identify joint dynamics, with MATLAB serving as the system identification tool. These methodologies were comparable to those described in Refs. [48–52]. Initially, closed-loop transfer functions were derived, and plant dynamics were obtained by algebraically rearranging the equations into open-loop form.

The dynamic behavior of each joint is determined by the resulting open-loop transfer functions, which are summarized in Eq. (1) and Table I. These parameters serve

as the foundation for robust control design under changing operating conditions. The discrete-time modeling approach enables the precise simulation and controller implementation of the RT3200 robotic platform.

$$P(z) = \frac{\gamma_1 z}{z^2 + \beta_1 z + \beta_0} \tag{1}$$

TABLE I. PARAMETERS USED IN THE OPEN-LOOP SYSTEM DYNAMICS

Joint	γ_1	$oldsymbol{eta}_1$	$oldsymbol{eta}_0$
Joint R	0.0333	-1.6871	0.6884
Joint T	0.0162	-1.7077	0.7111
Joint Z	0.0140	-1.7519	0. 526

B. PID Control System

The Proportional-Integral-Derivative (PID) controller is composed of a proportional term (K_p) , an integral term (K_i) , and a derivative term (K_d) . The continuous-time form is discretized when the algorithm is implemented on a microcontroller. The discrete-time transfer function used in Simulink, as illustrated in Fig. 2, can be expressed as Eqs. (2)–(4).

$$C(z) = K_p + \frac{\kappa_i T_s}{z - 1} + \frac{\kappa_d N}{1 + N T_s \frac{1}{z - 1}}$$
 (2)

$$U(z) = C(z) \cdot E(z) \tag{3}$$

$$E(z) = R(z) - Y(z) \tag{4}$$

where C(z) is the controller transfer function in the z-domain, T_s is the sampling interval, N is the derivative-filter coefficient, and z is the complex variable that represents discrete time, R(z) denotes the reference input, Y(z) represents the system output, E(z) is the difference between the desired and actual output, and the control signal U(z), computed as $C(z) \cdot E(z)$, is applied to the plant to minimize the tracking error.

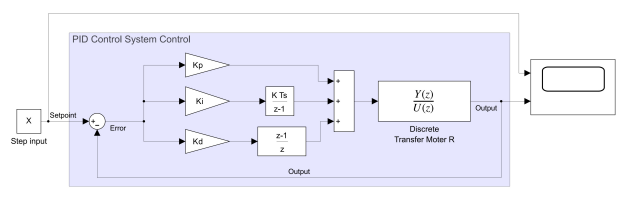


Fig. 2. Simulink model of the PID system.

The Ziegler-Nichols ultimate-gain method was employed to achieve the initial gains, which were subsequently refined through manual fine-tuning to align with the rise-time and overshoot objectives of each joint. The final gain values are presented in Table II.

However, the steady-state error is eliminated by the minor integral terms, while the proportional action dominates the response. A first-order filter with coefficient *N* is retained to attenuate measurement noise, and derivative action was set to zero.

TABLE II: PARAMETERS USED IN PID CONTROL

Joint	K_p	K _i	K_d
Joint R	1.000	0.015	0.000
Joint T	1.500	0.500	0.000
Joint Z	1.350	0.100	0.000

C. Expert-Rule-Based Gain Adjustment for PID Control

The control parameters are dynamically adjusted by the expert system to guarantee an effective response to step input signals. The system's logical conditions, as illustrated in Figs. 3 and 4, determine the appropriate adjustment values (output_for_adjust) based on the absolute value of the input (abs(input)). This is implemented in Simulink, as demonstrated in Fig. 5.

This method guarantees precise control during step disturbances by selecting appropriate gain values that are derived from the expert system in Fig. 3. The expert system logic is integrated into the corresponding Simulink model of the PID expert system for step input control, allowing for the real time computation of control parameters. This guarantees that the system reacts precisely to abrupt input modifications.

Fig. 3. Expert system for K_p adjustment under step input conditions.

The expert system for seamless function control is dedicated to the management of progressive input variations to guarantee a consistent and stable response. The structure of the system is analogous to that of the step input expert system, as illustrated in Fig. 4. However, it has been refined to accommodate continuous input signals. In response to the input's progressive fluctuation, the adjustment values (output_for_adjust) are dynamically computed.

```
1 1. Read input signal
2 2. Compute absolute_input = absolute value of input
3
4 3. If absolute_input >= 0 and absolute_input < 1 then
5 output for_adjust = 80.00
6 Else if absolute_input >= 1 and absolute_input < 2 then
7 output_for_adjust = 100.00
8 Else if absolute_input >= 2 and absolute_input < 3 then
9 output_for_adjust = 130.00
10 Else if absolute_input >= 3 and absolute_input < 4 then
11 output_for_adjust = 160.00
12 Else if absolute_input >= 4 then
13 output_for_adjust = 200.00
```

Fig. 4. Expert system for K_p adjustment under smooth function conditions.

The Simulink implementation of the PID expert system for both step and continuous function control is depicted in Fig. 5. This model demonstrates the system's capacity to maintain stability and minimize oscillations by utilizing PID control logic to process a variety of inputs.

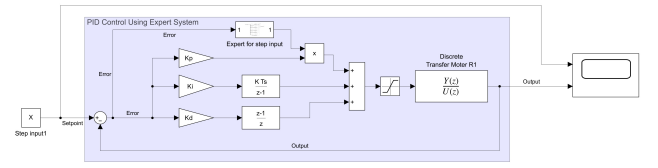


Fig. 5. PID expert system in Simulink for step or smooth inputs.

As shown in Fig. 5, the operation of the expert system for adjusting K_p is described by Eq. (5), where the proportional gain is modulated based on the expert output (output for adjust) according to input characteristics.

$$C(z) = K_p \cdot (output_for_adjust) + \frac{\kappa_i T_s}{z-1} + \frac{\kappa_d N}{1 + NT_s \frac{1}{z-1}}$$
 (5)

The dual expert control system dynamically transitions between step and smooth input expert systems in response to input characteristics, thereby integrating the benefits of both. The error setpoint (*Error_setpoint(k)*) is determined by the difference between the current and previous setpoints, as illustrated in Fig. 6. The system subsequently determines the appropriate control strategy based on the type of input variation. The final control output (*Control_Output*) is determined by summing the outputs of both expert systems.

Fig. 6. Expert system logic for dual PID expert control.

The Simulink model for dual expert control based on PID is depicted in Fig. 7. This configuration facilitates the seamless transition between step and smooth input control strategies by integrating both expert systems into a unified framework. By assessing the input characteristics in real time, the system identifies the most appropriate control approach to ensure optimal performance.

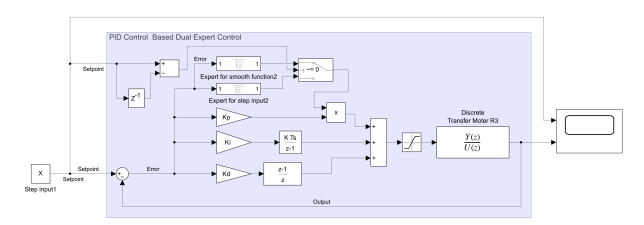


Fig. 7. Simulink model of PID-based dual expert control.

D. Fuzzy Logic Control System

The foundational framework of the fuzzy PD controller is established by Refs. [33, 68], which also demonstrate the adaptability of fuzzy logic in autonomous system control. The system proposed in this section is supported by these studies, which emphasize the integration of Mamdani

inference and Simulink implementation, resulting in precise and consistent motor control.

The fuzzy PD controller system functions by using nonlinear modifications derived from the error and its derivative to attain accurate control. The system's response is based on fuzzy logic principles, with the output estimate utilizing the centroid defuzzification approach as indicated in Eq. (6):

$$y_{\text{mam}}(x_i) = \frac{\sum_i \mu(x_i) x_i}{\sum_i \mu(x_i)}$$
 (6)

This approach computes the center of gravity of the fuzzy set along the x-axis, where $\mu(x_i)$ denotes the membership value of each point x_i inside the universe of discourse, as shown in Eq. (7):

$$e(k) = \operatorname{setpoint}(k) - \operatorname{output}(k)$$
 (7)

The control system employs the error signal e(k), which is defined as the discrepancy between the planned setpoint and the actual system output at step k, as shown in Eq. (8):

$$\dot{e}(k) = e(k) - e(k-1)$$
 (8)

The derivative of the error $\dot{e}(k)$ is calculated as the difference between the current error and the preceding error, offering dynamic feedback for modifications, as shown in Eq. (9):

$$U(k) = f(KFI \times e(k), KFI \times \dot{e}(k)) \times KFO$$
 (9)

The control signal U(k), produced at time step k, is a nonlinear function of the scaled error $KFI \times e(k)$ and the scaled derivative $KFI \times \dot{e}(k)$. The gain factor KFO also modifies the signal, indicating the output scaling.

These equations form the foundation of the fuzzy PD controller, as illustrated in Fig. 8, allowing adaptive and accurate regulation by dynamically reacting to variations in error and error rate. This framework facilitates robust performance under diverse operating conditions, guaranteeing stability and precision in system functionality.

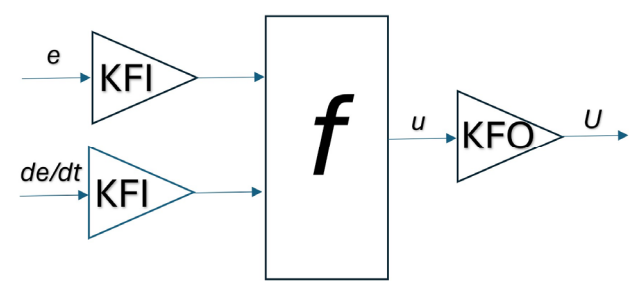


Fig. 8. Fuzzy logic controller design diagram.

The Fuzzy Logic Control (FLC) system utilizes approximate reasoning to regulate processes and generate appropriate solutions for diverse applications. It has been extensively studied and applied due to its versatility and

resilience. The Mamdani method is a commonly used technique for estimating fuzzy control outputs in robotic arm motor control, as shown in Fig. 9.

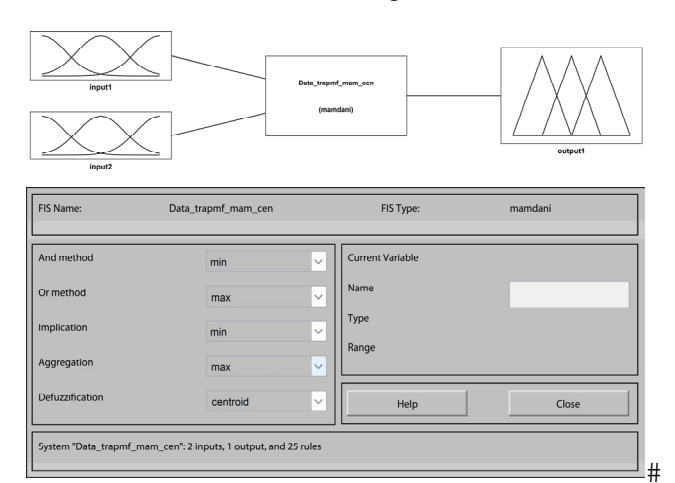


Fig. 9. Fuzzy logic designer (rule editor).

As shown in Fig. 10, fuzzy logic is incorporated into Simulink to effectively model and simulate control operations. The system uses two input signals: input signal 1 represents the error, and input signal 2 indicates the change in error. Each input includes five membership functions ranging from -1 to 1, allowing precise control and flexibility.

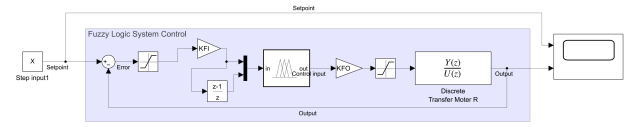


Fig. 10. Simulink model implementing fuzzy logic control.

The system output is defined by nine membership functions, also ranging from -1 to 1, enabling fine modulation of control responses. Table III provides a detailed explanation, and Fig. 11 illustrates the membership functions.

Fig. 12 illustrates the operation of the fuzzy logic control system using the FLC surface viewer, highlighting the relationship between input and output variables through a three-dimensional graphical depiction.

The fuzzy PD controller uses nonlinear adjustments based on the error and its derivative, with clearly defined saturation limits and scaling factors to ensure precision. The input values for joints R, T, and Z are constrained by saturation bounds. As shown in Fig. 5, Joint R is limited to –40 to 40, Joint T to –15 to 15, and Joint Z to –20 to 20. *KFI* defines the error range, setting the fuzzy input scaling factors to 1/40 for Joint R, 1/15 for Joint T, and 1/20 for Joint Z. The control input saturation limit for all three joints is set between –100 and 100, with a scaling factor of 100 defined by *KFO*. These parameters guarantee that the system operates within physical constraints, thereby maintaining precision and stability under varying conditions. All parameter values were determined by the optimization procedure outlined in the study optimizing

membership function tuning for fuzzy control of robotic manipulators using PID-driven data techniques [33, 68].

TABLE III. MEMBERSHIP FUNCTIONS OF FUZZY LOGIC CONTROLLER

Data Input			Input	I, f(e)		
	-	NB	NS	ZO	PS	PB
	NB	NM	NS	NM	PS	PM
Innut II #(da)	NS	NB	NM	NS	PM	PB
Input II, f(de)	ZO	VNB	NB	ZO	PB	VPB
	PS	NB	NM	PS	PM	PB
	PB	NM	NS	PM	PS	PM

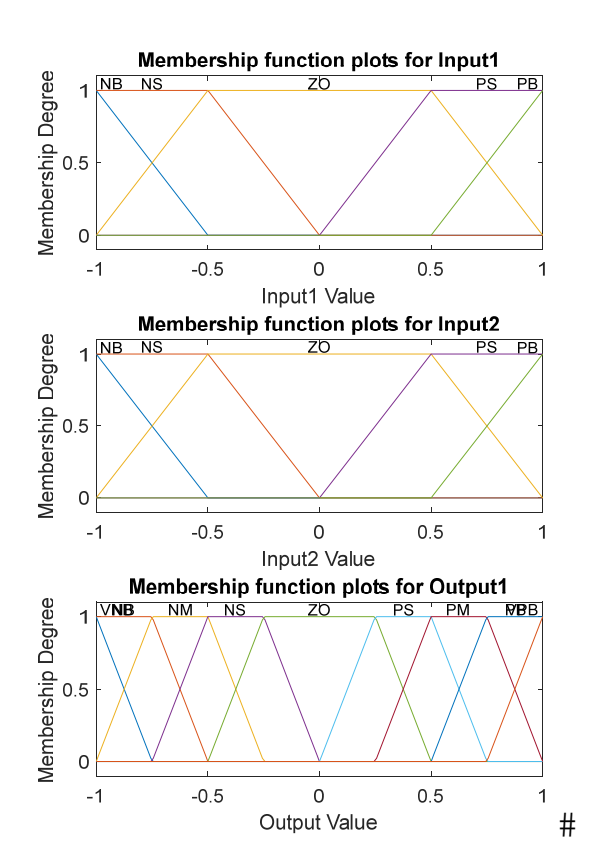


Fig. 11. Trapezoidal membership functions of Input 1, Input 2, and Output.

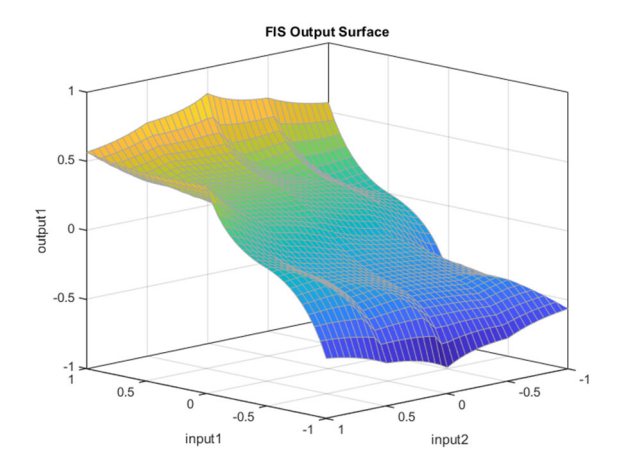


Fig. 12. FLC surface viewer showing the relationship between inputs and output.

E. Expert-Rule-Based Gain Adjustment for Fuzzy Control

A dual expert system, similar in structure to that used in PID control as described in Section C, is implemented to enhance the adaptability of fuzzy logic controllers in handling both abrupt and gradual input variations. The key difference lies in the target of adjustment: while the logic remains structurally consistent, the expert system in the fuzzy control framework modifies the output scaling factor (output for adjust) instead of adjusting PID gains.

To produce a stronger control response, the expert system increases the fuzzy scaling factor when it detects step-like inputs, as illustrated in Figs. 13 and 14. In contrast, the system reduces the scaling factor during steady input conditions to prevent unnecessary oscillations, which can be observed in Figs. 15 and 16. The switching logic and decision-making process are embedded within the fuzzy control framework and follow the approach outlined in Section III.C and illustrated in Fig. 6.

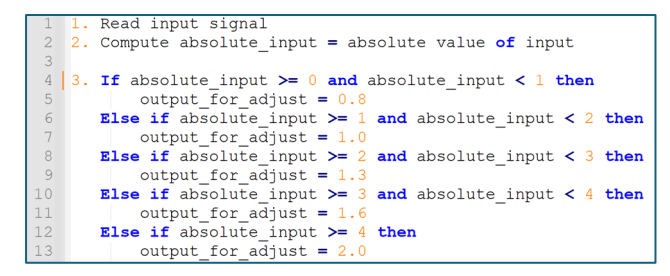


Fig. 13. Expert system logic for fuzzy control under step input conditions.

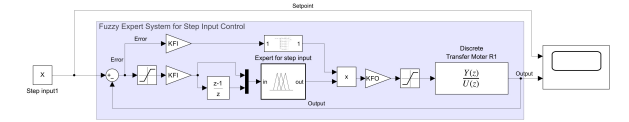


Fig. 14. Simulink model of fuzzy expert system for step input control.

Fig. 15. Expert system logic for fuzzy control under smooth function conditions.

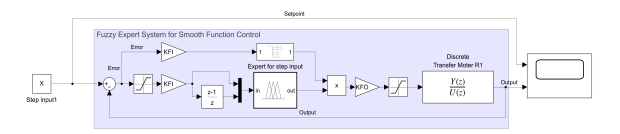


Fig. 16. Simulink model of fuzzy expert system for smooth function control.

Fig. 17 illustrates the comprehensive dual expert control system based on fuzzy logic. It continuously monitors the nature of the input signal and adjusts the fuzzy output in

real time using the expert-derived scaling factors. This integration enables the fuzzy controller to preserve its flexibility, stability, and robustness across a variety of dynamic environments.

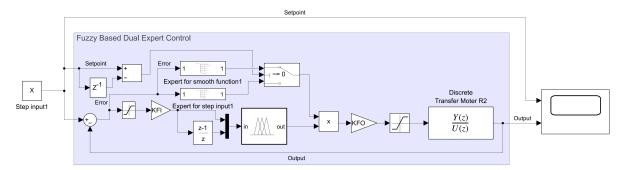


Fig. 17. Simulink model of fuzzy-based dual expert control.

As shown in Fig. 17, the operation of the expert system for adjusting $f(KFI \times e(k), KFI \times \dot{e}(k))$ is described by Eq. (10), where the proportional gain is modulated based on the expert output (output for adjust) according to input characteristics.

$$U(k) = f(KFI \times e(k), KFI \times \dot{e}(k)) \times (output_{for_{adjust}}) \times KFO \quad (10)$$

IV. RESULTS AND DISCUSSION

The results of the system simulations, which encompass the PID controller simulation, fuzzy logic controller simulation, and the overall comparative analysis, are presented in this section. The performance differences and overall effectiveness of each set of results are highlighted in an integrated discussion that follows the analysis of each set separately.

A. Results of Simulation PID Controller

The dynamic performance of the four PID-based schemes, namely conventional PID, step-input expert PID (PESC-Step), smooth-input expert PID (PESC-Smooth), and the proposed dual-expert PID (PBDEC), is summarized in Figs. 18 - 21and quantified Tables IV-XII. The classical PID eliminates overshoot at the expense of sluggish convergence, while PESC Step yields the shortest settling times ranging from 0.60 to 1.21 s by momentarily amplifying the proportional gain for modest step commands of 10 mm, 3.75°, and 5 mm for Joints R, T, and Z, respectively, as shown in Fig. 19 and Tables IV-VI. In this discrete-step regime, PESC Smooth over-reacts, producing an overshoot of up to 77% in Joint R because its gains are calibrated for gradual trajectories. In contrast, PBDEC combines the two expert rules in real time, ensuring that overshoot is limited to less than 24% and achieving the lowest IAE and RMSE in Joints R and Z, demonstrating the advantages of adaptive switching even for minor set-point jumps.

When the reference amplitudes are tripled to values of 30 mm, 11.25°, and 15 mm, as illustrated in Fig. 20 and relative Tables VII–IX, the ordering changes. PESC Smooth now tracks the larger steps with the smallest RMSE in Joints R and Z, but this comes at the expense of a 20% overshoot. PBDEC once again provides the most balanced response, maintaining an overshoot of under 9% in Joint R and achieving the best combined IAE-RMSE pair in Joints T and Z; this suggests that the decision logic correctly identifies the excitation as a step and selects the appropriate gain schedule. The conventional PID continues to demonstrate minimal overshoot yet suffers the largest cumulative error, confirming that fixed gains cannot simultaneously satisfy both speed and accuracy when set-point magnitudes vary considerably.

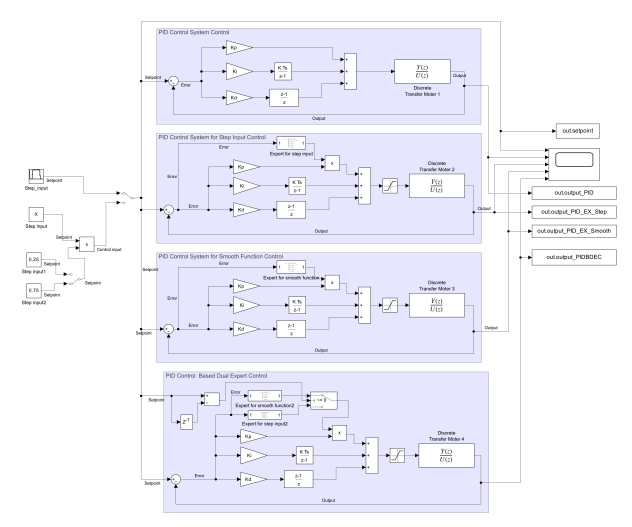


Fig. 18. Simulink block diagram overview for robotic system simulation using PID control.

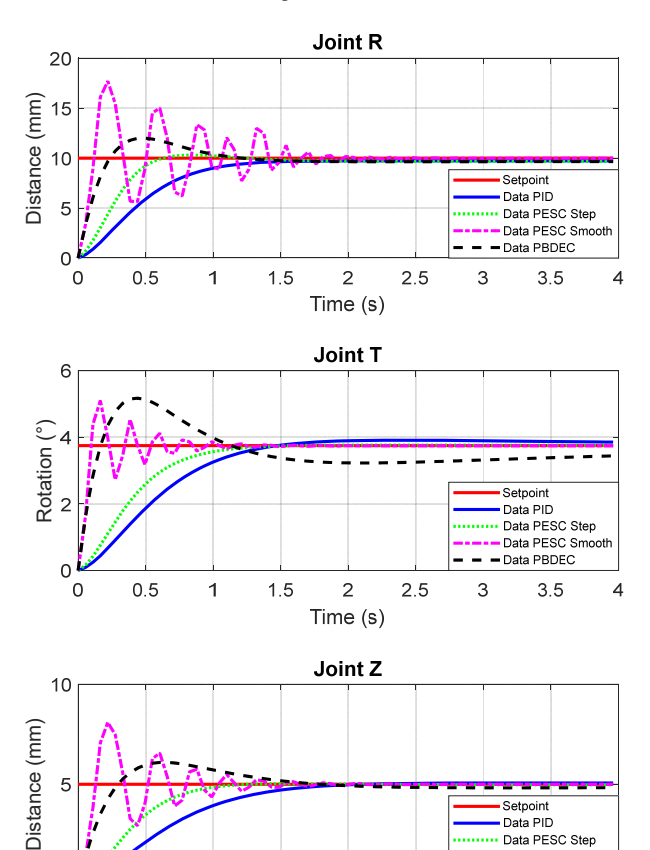


Fig. 19. System response for setpoints of joints R, T, and Z at 10, 3.75, and 5 using PID control.

2

Time (s)

Data PESC Step

Data PESC Smooth

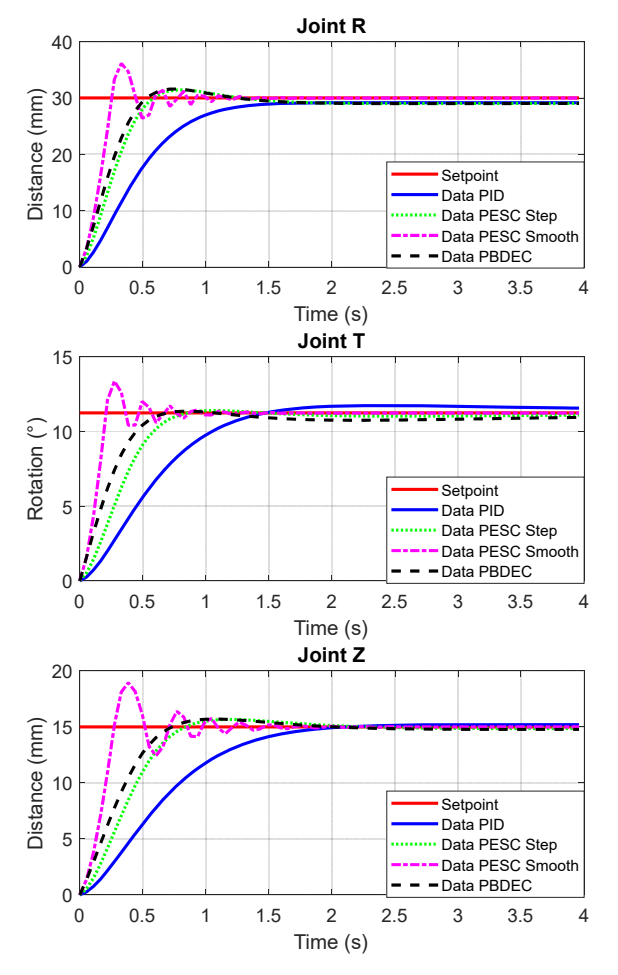


Fig. 20. System response for setpoints of joints R, T, and Z at 30, 11.25, and 15 using PID control.

The greatest benefit of expert scheduling appears in continuous, smooth trajectories, depicted in Fig. 21 and detailed in Tables X–XII. PESC Smooth tracks the ramp profile nearly perfectly, with RMSE values of only 0.31 mm, 0.096°, and 0.15 mm for Joints R, T, and Z, respectively. PBDEC closely follows, incurring a modest accuracy penalty from occasional switching, but still surpasses the classical PID by an order of magnitude. PESC Step, which is designed for discontinuities, continues to outperform the fixed-gain baseline despite exhibiting modest oscillations. These trends confirm that it is essential to reduce the gain during low-slope intervals in order to mitigate oscillations and limit steady-state deviation.

In general, the PBDEC configuration offers the most consistent performance across all test categories. By integrating the complementary strengths of the step- and smooth-specific expert rules, it achieves rapid rise times that are comparable to PESC-Step during abrupt changes, while also approaching the low-error behavior of PESC-Smooth on incremental trajectories. Consequently, the dual-expert strategy offers a resilient and adaptable solution for robotic manipulators that operate in environments with unpredictable perturbation characteristics and reference profiles, as illustrated in Figs. 18–21.

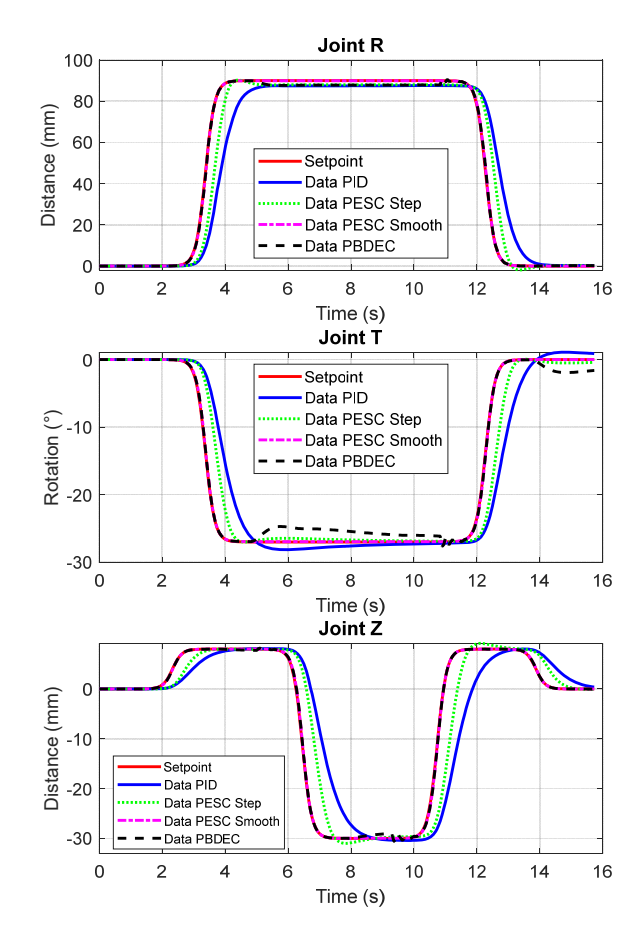


Fig. 21. System response to smooth input for joints R, T, and Z using PID control.

TABLE IV. PERFORMANCE METRICS FOR JOINT R AT SETPOINT 10 USING PID CONTROL

Туре	Setting Time (s)	%OS (%)	Rise time (s)	IAE (mm)	RMSE (mm)
Data_PID	1.81	0.01	1.26	6.00	2.90
Data_PESC_Step	0.60	6.35	0.55	3.78	2.27
Data PESC Smooth	1.98	77.14	0.11	5.15	2.45
Data PBDEC	1.21	24.41	0.22	3.19	1.64

TABLE V. PERFORMANCE METRICS FOR JOINT T AT SETPOINT 3.75 USING PID CONTROL

Туре	Setting Time (s)	%OS (%)	Rise time (s)	IAE (°)	RMSE (°)
Data_PID	3.85	1.21	1.26	2.53	1.17
Data_PESC_Step	1.21	0.16	0.99	1.67	0.99
Data_PESC_Smooth	0.93	36.26	0.11	0.70	0.56
Data_PBDEC	1.15	51.82	0.16	2.31	0.77

TABLE VI. PERFORMANCE METRICS FOR JOINT Z AT SETPOINT 5 USING PID CONTROL

Туре	Setting Time (s)	%OS (%)	Rise time (s)	IAE (mm)	RMSE (mm)
Data PID	1.76	0.02	1.59	3.59	1.68
Data_PESC_Step	0.99	1.08	0.93	2.20	1.33
Data PESC Smooth	1.50	62.14	1.60	1.80	1.02
Data PBDEC	1.81	26.31	0.27	1.91	0.90

TABLE VII. PERFORMANCE METRICS FOR JOINT R AT SETPOINT 30 USING PID CONTROL

Туре	Setting Time (s)	%OS (%)	Rise time (s)	IAE (mm)	RMSE (mm)
Data_PID	1.70	0.01	1.32	18.01	8.70
Data_PESC_Step	1.04	8.23	0.55	11.51	6.81
Data_PESC_Smooth	0.82	20.50	0.22	7.06	5.71
Data PBDEC	0.99	8.83	0.49	6.30	6.30

TABLE VIII. PERFORMANCE METRICS FOR JOINT T AT SETPOINT 11.25
USING PID CONTROL

Туре	Setting Time (s)	%OS (%)	Rise time (s)	IAE (°)	RMSE (°)
Data_PID	3.85	1.21	1.26	7.59	3.52
Data_PESC_Step	0.71	2.90	0.71	4.47	2.78
Data PESC Smooth	0.77	19.04	0.16	2.28	1.98
Data_PBDEC	3.68	4.12	0.55	4.00	2.30

TABLE IX. PERFORMANCE METRICS FOR JOINT Z AT SETPOINT 15
USING PID CONTROL

Туре	Setting Time (s)	%OS (%)	Rise time (s)	IAE (mm)	RMSE (mm)
Data_PID	1.70	0.02	1.59	10.78	5.04
Data_PESC_Step	1.59	5.48	0.71	6.61	3.95
Data PESC Smooth	1.21	26.34	0.27	4.28	3.02
Data_PBDEC	1.48	6.24	0.66	5.61	3.46

TABLE X. PERFORMANCE METRICS FOR JOINT R UNDER SMOOTH INPUT USING PID CONTROL

Type	IAE (mm)	RMSE (mm)
Data_PID	107.49	13.95
Data_PESC_Step	62.24	8.82
Data_PESC_Smooth	1.73	0.31
Data_PBDEC	14.41	1.33

TABLE XI. PERFORMANCE METRICS FOR JOINT T UNDER SMOOTH INPUT USING PID CONTROL

Type	IAE (°)	RMSE (°)
Data_PID	37.15	4.81
Data_PESC_Step	21.26	3.24
Data PESC Smooth	0.78	0.096
Data PBDEC	12.49	1.11

TABLE XII. PERFORMANCE METRICS FOR JOINT Z UNDER SMOOTH INPUT USING PID CONTROL

Type	IAE (mm)	RMSE (mm)
Data_PID	66.41	7.77
Data_PESC_Step	37.67	5.13
Data PESC Smooth	0.88	0.15
Data_PBDEC	2.11	0.26

B. Results of Simulation Fuzzy Logic Controller

The fuzzy-logic experiments were implemented using the Simulink architecture depicted in Fig. 22, which was structured into three tiers: continuous trajectory, enlarged step commands of 30 mm, 11.25° , and 15 mm, and modest step commands of 10 mm, 3.75° , and 5 mm. The baseline FLC, the step-input fuzzy expert (FESC-Step), the smooth-input fuzzy expert (FESC-Smooth), and the dual-expert fuzzy controller (FBDEC) were all benchmarked. Tables XIII–XXI present numerical indicators, while Figs. 23–25 illustrate critical responses.

Fuzzy Logic-based Dual Expert Controller (FBDEC) attained the optimal balance between speed and accuracy for reference values of 10 mm, 3.75°, and 5 mm. The overshoot in Joint R was maintained at 2.59%, a significantly lower value than that of FLC at 4.51% and FESC-Smooth at 9.13%. Additionally, the ascent periods were comparable to those of the faster FESC-Step. The overall precision was reduced by the increased excess, despite the fact that FESC-Step decreased the settling time to 0.77 s in Joint R. These results verify that the adaptive switching in FBDEC effectively reduces excessive excursions during low-amplitude disturbances without compromising responsiveness.

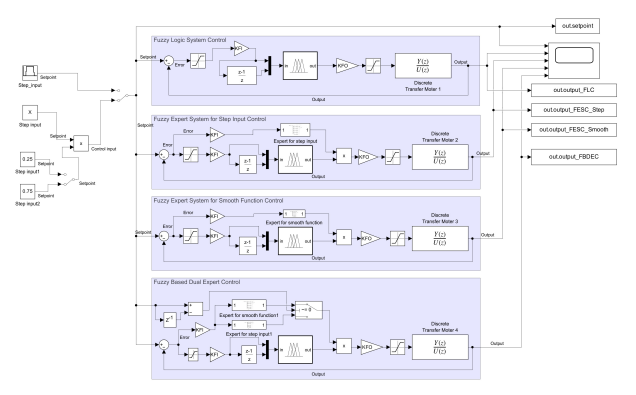


Fig. 22. Simulink block diagram overview for robotic system simulation using fuzzy logic control.

The monitoring priorities underwent a transformation as the command magnitudes were increased threefold. FESC-Smooth capitalized on its higher steady-state gain to attain the lowest RMSE in Joints R and Z; however, it resulted in an overshoot of approximately 20%. FBDEC once again attained the most balanced outcome, as the combined IAE-RMSE scores in Joints T and Z were the best overall, and overshoot remained below 9% in Joint R. The pure FLC maintained minimal overshoot but accrued the largest integrated errors, underscoring the limitation of fixed gains across diverse set-point scales.

In joints R, T, and Z, FESC-Smooth achieved RMSE values of 0.31 mm, 0.096°, and 0.15 mm, respectively, with continuous input. FBDEC followed closely, incurring a modest accuracy penalty from intermittent rule switching, but still outperformed FLC by approximately an order of magnitude. Despite minor oscillations, FESC-Step outperformed the baseline, indicating that expert scheduling offers advantages that extend beyond its primary design envelope.

Fuzzy Logic-based Dual Expert Controller (FBDEC) demonstrated the most consistent performance in all test categories. It confirmed the efficacy of real-time rule selection by combining the brief settling times of FESC-Step during abrupt changes with the low steady-state error of FESC-Smooth on gradual profiles. The dual-expert fuzzy architecture offers a resilient and adaptable solution for manipulators that are required to manage external disturbances and unpredictable reference shapes, as demonstrated in Figs. 23–25 and Tables XIII–XXI.

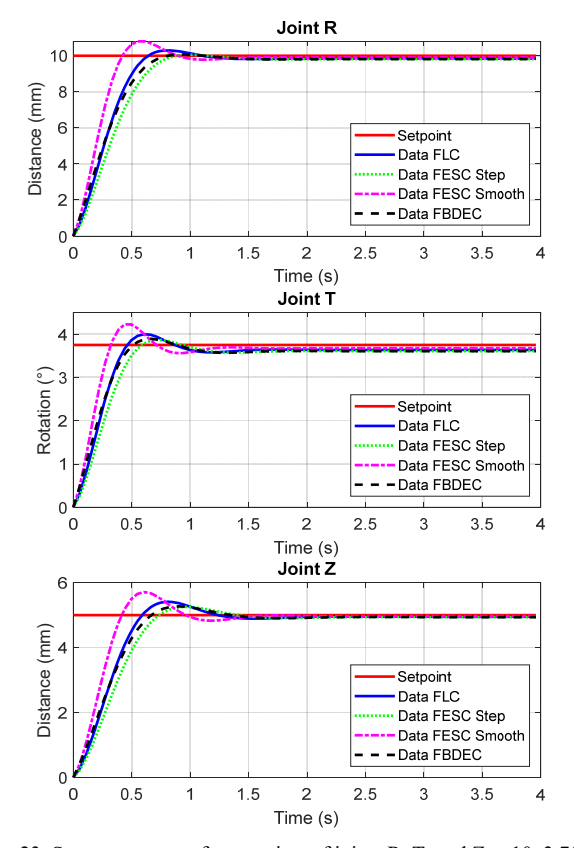


Fig. 23. System response for setpoints of joints R, T, and Z at 10, 3.75, and 5 using fuzzy logic control.

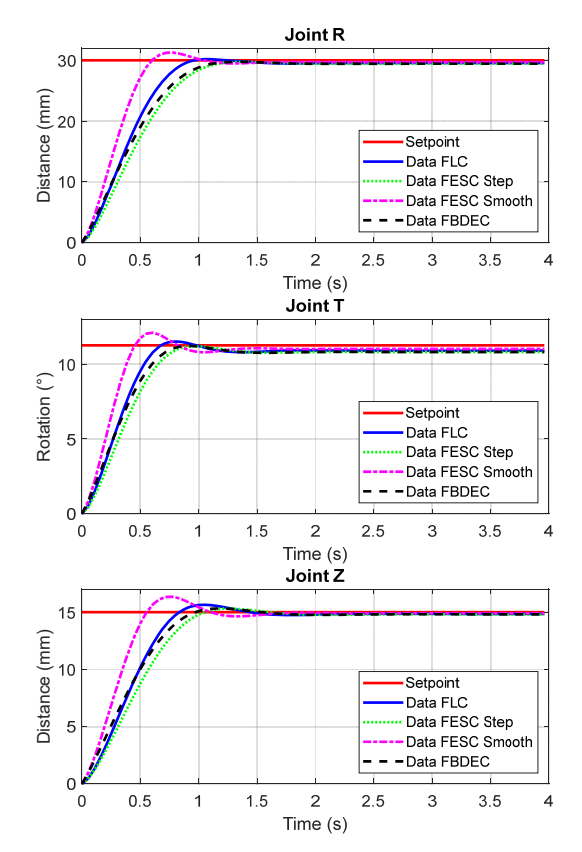


Fig. 24. System response for setpoints of joints R, T, and Z at 30, 11.25, and 15 using fuzzy logic control.

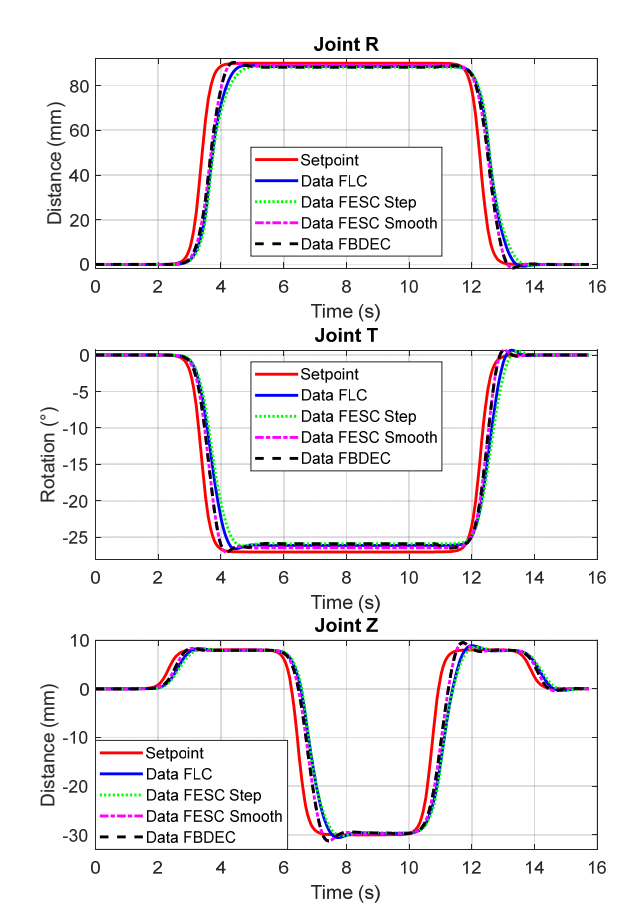


Fig. 25. System response to smooth input for joints R, T, and Z using Fuzzy logic control.

TABLE XIII. PERFORMANCE METRICS FOR JOINT R AT SETPOINT 10 USING FUZZY LOGIC CONTROL

Туре	Setting Time (s)	%OS (%)	Rise time (s)	IAE (mm)	RMSE (mm)
Data_FLC	0.55	4.51	0.44	3.55	2.31
Data_FESC_Step	0.77	2.44	0.55	4.12	2.50
Data_FESC_Smooth	0.80	9.13	0.28	2.83	2.04
Data_FBDEC	0.71	2.59	0.50	3.63	2.27

TABLE XIV. PERFORMANCE METRICS FOR JOINT T AT SETPOINT 3.75 USING FUZZY LOGIC CONTROL

Туре	Setting Time (s)	%OS (%)	Rise time (s)	IAE (°)	RMSE (°)
Data_FLC	1.32	9.97	0.28	1.35	0.80
Data_FESC_Step	1.70	7.18	0.39	1.54	0.86
Data FESC Smooth	0.99	14.99	0.28	1.10	0.71
Data_FBDEC	1.69	7.87	0.39	1.37	0.77

TABLE XV. PERFORMANCE METRICS FOR JOINT Z AT SETPOINT SETPOINT 5 USING FUZZY LOGIC CONTROL

Type	Setting Time (s)	%OS (%)	Rise time (s)	IAE (mm)	RMSE (mm)
Data_FLC	1.10	9.23	0.44	1.87	1.19
Data FESC Step	1.25	6.36	0.50	2.10	1.27
Data_FESC_Smooth	1.26	14.95	0.28	1.56	1.06
Data_FBDEC	1.15	6.68	0.44	1.86	1.16

TABLE XVI. PERFORMANCE METRICS FOR JOINT R AT SETPOINT SETPOINT 30 USING FUZZY LOGIC CONTROL

Туре	Setting Time (s)	%OS (%)	Rise time (s)	IAE (mm)	RMSE (mm)
Data_FLC	0.82	2.16	0.61	13.73	8.06
Data_FESC_Step	1.10	1.02	0.77	16.46	8.72
Data_FESC_Smooth	0.88	5.34	0.39	10.49	7.04
Data FBDEC	1.04	1.02	0.77	15.13	8.17

TABLE XVII. PERFORMANCE METRICS FOR JOINT T AT SETPOINT SETPOINT 11.25 USING FUZZY LOGIC CONTROL

Туре	Setting Time (s)	%OS (%)	Rise time (s)	IAE (°)	RMSE (°)
Data_FLC	0.60	5.54	0.44	4.86	2.76
Data FESC Step	1.81	3.60	0.61	5.72	2.97
Data FESC Smooth	0.77	9.79	0.33	3.81	2.43
Data_FBDEC	1.80	3.68	0.55	5.24	2.75

TABLE XVIII. PERFORMANCE METRICS FOR JOINT Z AT SETPOINT SETPOINT 15 USING FUZZY LOGIC CONTROL

Туре	Setting Time (s)	%OS (%)	Rise time (s)	IAE (mm)	RMSE (mm)
Data_FLC	1.21	5.35	0.55	6.95	4.11
Data_FESC_Step	0.98	3.36	0.66	7.80	4.34
Data_FESC_Smooth	0.99	9.73	0.39	5.31	3.51
Data_FBDEC	0.93	3.42	0.66	6.87	3.96

TABLE XIX. PERFORMANCE METRICS FOR JOINT R UNDER SMOOTH INPUT USING FUZZY LOGIC CONTROL

Type	IAE (mm)	RMSE (mm)
Data_FLC	70.14	10.31
Data_FESC_Step	80.48	11.18
Data_FESC_Smooth	52.50	8.37
Data FBDEC	57.49	8.42

TABLE XX. PERFORMANCE METRICS FOR JOINT T UNDER SMOOTH INPUT USING FUZZY LOGIC CONTROL

Type	IAE (°)	RMSE (°)
Data_FLC	20.75	2.64
Data_FESC_Step	25.75	3.13
Data FESC Smooth	13.32	1.80
Data_FBDEC	16.56	1.89

TABLE XXI. PERFORMANCE METRICS FOR JOINT Z UNDER SMOOTH INPUT USING FUZZY LOGIC CONTROL

Type	IAE (mm)	RMSE (mm)
Data_FLC	32.70	4.75
Data FESC Step	35.05	4.96
Data_FESC_Smooth	23.84	3.64
Data FBDEC	24.23	3.64

C. Over All Results of Simulation

The most balanced and robust performance across all test scenarios is routinely achieved by dual-expert architectures, namely PBDEC for PID and FBDEC for fuzzy logic, as revealed by the comparative analysis of all control strategies under step and smooth input conditions. The conventional PID was substantially outperformed by PBDEC in step commands of 10 mm, 3.75°, and 5 mm, as it improved both IAE and RMSE values and reduced overshoot. In the same vein, FBDEC surpassed the baseline FLC by maintaining overshoot of Joint R below 3%, achieving comparable rise times to the step-tuned

expert, and maintaining higher tracking accuracy than FESC-Smooth. When contrasted with earlier fuzzy-PID studies such as Ref. [7], which continue to exhibit noticeable overshoot and lengthy settling under similar abrupt inputs, FBDEC consistently trends toward smaller peak excursions and faster stabilization, underscoring the benefit of rule-based adaptation.

Both PBDEC and FBDEC maintained their exceptional adaptability when confronted with enlarged step inputs of 30 mm, 11.25°, and 15 mm. The RMSE in Joints T and Z was minimized by FBDEC, despite a modest increase in rise time. In Joint R, PBDEC attained the lowest combined error metrics and contained overshoot within 9%. Conversely, the fixed-gain PID and FLC controllers exhibited the most limited adaptability to diverse input scales and the highest accumulated errors. Likewise, PSO-PID frameworks described in Ref. [23] focus on reducing integrated error through a single optimized gain set; by contrast, PBDEC retains low cumulative error while simultaneously suppressing overshoot, illustrating the additional advantage gained from on-the-fly gain-set switching rather than offline retuning.

Adaptive switching works even better when the input are stable. The smooth-specific experts (PESC-Smooth and FESC-Smooth) are almost as good as the dual-expert controllers. On the other hand, the fixed-gain controllers are much worse. When working on smooth paths, PESC-Smooth and FESC-Smooth have the lowest RMSE of all the joints, but they both have considerable difficulty under step conditions. PBDEC and FBDEC effectively mitigate this limitation by employing context-aware rule switching, which enables a generalized and reliable control response. Collectively, these trend-level observations in relation to Refs. [7, 23] underscore the simultaneous enhancements in transient attenuation and steady-state precision that dynamic gain scheduling provides, despite the fact that the underlying plant models differ.

In conclusion, the dual-expert approaches demonstrate precision, adaptability, and resilience across a wide range of input profiles, thereby verifying their appropriateness for robotic manipulators operating in dynamic environments. The proposed architecture is intended to be positioned within the broader control-strategy landscape without implying a direct numerical comparison, and the cross-study contrasts presented here are qualitative rather than quantitative.

V. CONCLUSION

In this research, a dual-expert gain-adaptation strategy was evaluated for robotic manipulators that are required to track both continuous trajectories and abrupt step commands. Two controllers were developed: PBDEC, which improves a PID loop by incorporating distinct gain tables for step and smooth inputs, and FBDEC, which applies the same principle to a fuzzy PD loop. The online switching between the two tables is solely determined by the reference-profile increment through a simple rule set. PBDEC reduced integral-absolute error and root-mean-square error by up to 46.9% in comparison to a

fixed-gain PID, while maintaining overshoot below 9%, as demonstrated by simulations conducted on a three-joint Seiko D-Tran RT3200 model. The tracking accuracy of FBDEC was comparable to that of a smooth-tuned fuzzy controller, and the overshoot was kept below 3% during ramp tracking; it did not exhibit the overshoot observed in the step-tuned fuzzy variant. Single-mode experts performed well only under the profile for which they were tailored, whereas the dual-expert approach maintained acceptable performance under both profiles. The switching logic can be implemented in existing programmable logic controllers or real-time-target hardware without additional sensors or plant identification, as it uses only reference information and two predefined gain tables. The method can accommodate both motion regimes without retuning on medical manipulators that transition between fast puncture and slow trajectory following, pick-and-place arms that alternate between rapid indexing and delicate insertion. The analysis was restricted to simulations with nominal plant parameters and a 1 kHz control cycle. Future work should test the algorithm on physical hardware, examine behaviour under parameter drift and external disturbances, and investigate automatic adjustment of the switching threshold to handle reference profiles that vary continuously between step and smooth cases.#

CONFLICT OF INTEREST

The authors declare no conflict of interest.

AUTHOR CONTRIBUTIONS

PC conceived the research idea and hypotheses, prepared the experiments, conducted simulations, analyzed the data, and critically reviewed the results. AW and PM contributed to hypothesis validation, experimental design, execution, data analysis, and manuscript drafting and revision. KR designed the apparatus structure, assisted with experiments, analyzed data, and verified results. AN supported manuscript evaluation and data interpretation. WK, PI, and RC assisted with data acquisition and provided guidance on manuscript preparation and revision. NT provided guidance on the theoretical context, critical evaluation, and research execution; all authors had approved the final version.

FUNDING

This research was funded by the Research Institute, Academic Services Center, and College of Biomedical Engineering, Rangsit University, under grant number RSUERB2025-006.

ACKNOWLEDGMENT

The researcher would like to thank the Ethics Review Board of Rangsit University for reviewing the project and certifying that the research does not involve human subjects. Moreover, AI-driven methods (QuillBot Premium) were utilized for grammatical verification, paraphrasing, and linguistic augmentation to ensure the accuracy and clarity of the text.

REFERENCES

- [1] E. S. Ghith and F. A. A. Tolba, "Design and optimization of PID controller using various algorithms for micro-robotics system," *Journal of Robotics and Control (JRC)*, vol. 3, no. 3, pp. 244–256, 2022. doi: 10.18196/jrc.v3i3.14827
- [2] H. Maghfiroh, A. Ramelan, and F. Adriyanto, "Fuzzy-PID in BLDC motor speed control using MATLAB/Simulink," *Journal of Robotics and Control (JRC)*, vol. 3, no. 1, pp. 8–13, 2021. doi: 10.18196/jrc.v3i1.10964
- [3] K. Vanchinathan and N. Selvaganesan, "Adaptive fractional order PID controller tuning for brushless DC motor using artificial bee colony algorithm," *Results in Control and Optimization*, vol. 4, 100032, 2021. doi: 10.1016/j.rico.2021.100032
- [4] R. P. Borase, D. K. Maghade, S. Y. Sondkar et al., "A review of PID control, tuning methods and applications," *International Journal of Dynamics and Control*, vol. 9, no. 2, pp. 818–827, 2020. doi: 10.1007/s40435-020-00665-4
- [5] M. A. Shamseldin, M. Araby, and S. El-Khatib, "A low-cost high performance electric vehicle design based on variable structure fuzzy PID control," *Journal of Robotics and Control (JRC)*, vol. 5, no. 6, pp. 1713–1721, 2024. doi: 10.18196/jrc.v5i6.22071
- [6] S. J. Hammoodi, K. S. Flayyih, and A. R. Hamad, "Design and implementation of speed control system for DC motor based on PID control and Matlab Simulink," *International Journal of Power Electronics and Drive Systems*, vol. 11, no. 1, pp. 127–134, 2020. doi: 10.11591/ijpeds.v11.i1.pp127-134
- [7] M. A. Abdelghany, A. O. Elnady, and S. O. Ibrahim, "Optimum PID controller with fuzzy self-tuning for DC servo motor," *Journal* of Robotics and Control (JRC), vol. 4, no. 4, pp. 500–508, 2023. doi: 10.18196/jrc.v4i4.18676
- [8] R. Askour, H. Jbari, and B. B. Idrissi, "Comparative investigation of DSP-based speed control of PMSM using proportional integral and Takagi-Sugeno fuzzy logic controller," *International Journal* of Electrical and Electronic Engineering & Telecommunications, vol. 13, no. 2, pp. 135–147, 2023. doi: 10.18178/ijeetc.13.2.135-147
- [9] N. T. Thinh, T. P. Tho, and N. D. X. Hai, "Adaptive fuzzy control for autonomous robot under complex environment," *International Journal of Mechanical Engineering and Robotics Research*, vol. 10, no. 5, pp. 216–223, 2021. doi: 10.18178/ijmerr.10.5.216-223
- [10] K. Eltag, M. S. Aslamx, and R. Ullah, "Dynamic stability enhancement using fuzzy PID control technology for power system," *International Journal of Control, Automation and Systems*, vol. 17, pp. 234–242, 2019. doi: 10.1007/s12555-018-0109-7
- [11] S. Nemmour, B. Daaou, and F. Okello, "Fuzzy control for spacecraft orbit transfer with gain perturbations and input constraint," *International Journal of Robotics and Control Systems*, vol. 4, no. 4, pp. 1561–1583, 2024. doi: 10.31763/ijrcs.v4i4.1549
- [12] A. J. Humaidi and H. A. Hussein, "Adaptive control of parallel manipulator in Cartesian space," in Proc. the 2019 IEEE International Conf. on Electrical, Computer and Communication Technologies (ICECCT), 2019, pp. 1–8. doi: 10.1109/ICECCT.2019.8869257
- [13] A. J. Humaidi, A. A. Oglah, S. J. Abbas et al., "Optimal augmented linear and nonlinear PD control design for parallel robot based on PSO tuner," *International Review on Modelling and Simulations*, vol. 12, no. 5, pp. 281–291, 2019. doi: 10.15866/iremos.v12i5.16298
- [14] S. M. Mahdi, A. I. Abdulkareem, A. J. Humaidi et al., "Comprehensive review of control techniques for various mechanisms of parallel robots," *IEEE Access*, 2025. doi: 10.1109/ACCESS.2025.3557937
- [15] A. R. Nasser, A. T. Azar, A. J. Humaidi et al., "Intelligent fault detection and identification approach for analog electronic circuits based on fuzzy logic classifier," *Electronics*, vol. 10, no. 23, 2888, 2021. doi: 10.3390/electronics10232888
- [16] H. Y. Abed, A. T. Humod, and A. J. Humaidi, "Type 1 versus type 2 fuzzy logic speed controllers for brushless DC motors," *International Journal of Electrical and Computer Engineering*, vol. 10, no. 1, pp. 265–274, 2020. doi: 10.11591/ijece.v10i1.pp265-274

- [17] Z. Yasmine, B. Karim, and R. Razika, "Adaptive fuzzy logic control of quadrotor," *International Journal of Robotics and Control Systems*, vol. 4, no. 4, pp. 2095–2118, 2024. doi: 10.31763/ijrcs.v4i4.1583
- [18] N. Ali, R. Ghazali, and A. Tahir, "Enhanced hybrid robust fuzzy-PID controller for precise trajectory tracking electro-hydraulic actuator system," *International Journal of Robotics and Control Systems*, vol. 4, no. 2, pp. 795–813, 2024. doi: 10.31763/ijrcs.v4i2.1407
- [19] S. Mahfoud, A. Derouich, N. El Ouanjli et al., "A new strategy-based PID controller optimized by genetic algorithm for DTC of the doubly fed induction motor," Systems, vol. 9, no. 2, 37, 2021. doi: 10.3390/systems9020037
- [20] M. M. Nishat, F. Faisal, A. J. Evan et al., "Development of Genetic Algorithm (GA) based optimized PID controller for stability analysis of DC-DC buck converter," *Journal of Power and Energy Engineering*, vol. 8, no. 9, 8, 2020. doi: 10.4236/jpee.2020.89002
- [21] H. Feng, C. B. Yin, W. W. Weng et al., "Robotic excavator trajectory control using an improved GA based PID controller," *Mechanical Systems and Signal Processing*, vol. 105, pp. 153–168, 2018. doi: 10.1016/j.ymssp.2017.12.014
- [22] Z. Qi, Q. Shi, and H. Zhang, "Tuning of digital PID controllers using particle swarm optimization algorithm for a CAN-Based DC motor subject to stochastic delays," *IEEE Transactions on Industrial Electronics*, vol. 67, no. 7, pp. 5637–5646, 2020. doi: 10.1109/TIE.2019.2934030
- [23] M. Setiawan, A. Ma'arif, M. Saifuddin et al., "A comparative study of PID, FOPID, ISF, SMC, and FLC controllers for DC motor speed control with particle swarm optimization," *International Journal of Robotics and Control Systems*, vol. 5, no. 1, pp. 640–660, 2025. doi: 10.31763/ijrcs.v5i1.1764
- [24] M. Singh, S. Arora, and O. Shah, "Enhancing hybrid power system performance with GWO-tuned fuzzy-PID controllers: A comparative study," *International Journal of Robotics and Control Systems*, vol. 4, no. 2, pp. 709–726, 2024. doi: 10.31763/ijrcs.v4i2.1388
- [25] C. Y. Kang, H. Nabipour, and H. S. Chua, "Design of Battery Energy Storage System (BESS) with fuzzy control for Pico hydro," *International Journal of Electrical and Electronic Engineering & Telecommunications*, vol. 11, no. 1, pp. 18–23, 2022. doi: 10.18178/ijeetc.11.1.18-23
- [26] S. Howimanporn, S. Chookaew, and C. Silawatchananai, "Real-time evaluation position control of directional wheel conveyor using fuzzy embedded PLC and SCADA," *International Journal of Mechanical Engineering and Robotics Research*, vol. 10, no. 6, pp. 328–336, 2021. doi: 10.18178/ijmerr.10.6.328-336
- [27] R. A. AL-Jarrah, "Hybrid fuzzy-PID closed loop to regulate quadcopter system," *International Journal of Mechanical Engineering and Robotics Research*, vol. 10, no. 9, pp. 469–477, 2021. doi: 10.18178/ijmerr.10.9.469-477
- [28] N. T. T. Hieu and N. T. Thinh, "Controlling water jet based on fuzzy controller for cleaning and massage patient's head," *International Journal of Mechanical Engineering and Robotics Research*, vol. 11, no. 9, pp. 646–652, 2022. doi: 10.18178/ijmerr.11.9.646-652
- [29] A. Ma'arif and A. Çakan, "Simulation and Arduino hardware implementation of DC motor control using sliding mode controller," *Journal of Robotics and Control (JRC)*, vol. 2, no. 6, pp. 582–589, 2021. doi: 10.18196/jrc.26140
- [30] P. Visavapiwong, S. Chookaew, and S. Howimanporn, "Parameter estimate PID controller for multi-position control of servo drive system with fuzzy self-tuning," *International Journal of Mechanical Engineering and Robotics Research*, vol. 13, no. 4, pp. 456–462, 2024. doi: 10.18178/ijmerr.13.4.456-462
- [31] A. Shuraiji and S. Shneen, "Fuzzy logic control and PID controller for brushless permanent magnetic direct current motor: A comparative study," *Journal of Robotics and Control (JRC)*, vol. 3, no. 6, pp. 762–768, 2022. doi: 10.18196/jrc.v3i6.15974
- [32] E. A. Nugroho, J. D. Setiawan, and M. Munadi, "Handling four DOF robot to move objects based on color and weight using fuzzy logic control," *Journal of Robotics and Control (JRC)*, vol. 4, no. 6, pp. 769–779, 2023. doi: https://doi.org/10.18196/jrc.v4i6.20087
- [33] P. Chotikunnan, R. Chotikunnan, A. Nirapai et al., "Optimizing membership function tuning for fuzzy control of robotic manipulators using PID-driven data techniques," *Journal of Robotics and Control (JRC)*, vol. 4, no. 2, pp. 128–140, 2023. doi: 10.18196/jrc.v4i2.18108

- [34] S. Singh and M. K. Sandhu, "Multi-level fuzzy inference system based handover decision model for unmanned vehicles," *International Journal of Electrical and Electronic Engineering & Telecommunications*, vol. 12, no. 1, pp. 35–45, 2023. doi: 10.18178/ijeetc.12.1.35-45
- [35] C. F. Riman and P. E. Abi-Char, "Fuzzy logic control for mobile robot navigation in automated storage," *International Journal of Mechanical Engineering and Robotics Research*, vol. 12, no. 5, pp. 313–323, 2023. doi: 10.18178/ijmerr.12.5.313-323
- [36] D. N. Minh, H. D. Quang, N. D. Phuong et al., "An adaptive fuzzy dynamic surface control tracking algorithm for mecanum wheeled mobile robots," *International Journal of Mechanical Engineering* and Robotics Research, vol. 12, no. 6, pp. 354–361, 2023. doi: 10.18178/ijmerr.12.6.354-361
- [37] P. M. Tuan, N. D. Tai, T. Q. Huy et al., "Flexible path planning of mobile robot for avoiding the dynamic obstacles using fuzzy controllers," *International Journal of Mechanical Engineering and Robotics Research*, vol. 13, no. 1, pp. 126–132, 2024. doi: 10.18178/ijmerr.13.1.126-132
- [38] C. F. Riman and P. E. Abi-Char, "Novel fuzzy reinforcement algorithm for mobile robot navigation in automated storage," *International Journal of Mechanical Engineering and Robotics Research*, vol. 13, no. 2, pp. 284–295, 2024. doi: 10.18178/ijmerr.13.2.284-295
- [39] P. T. Phuc, T. P. Tho, N. D. X. Hai et al., "Design of adaptive fuzzy sliding mode controller for mobile robot," *International Journal of Mechanical Engineering and Robotics Research*, vol. 10, no. 2, pp. 54–59, 2021. doi: 10.18178/ijmerr.10.2.54-59
- [40] D. T. Tran, N. M. Hoang, N. H. Loc et al., "A fuzzy LQR PID control for a two-legged wheel robot with uncertainties and variant height," *Journal of Robotics and Control (JRC)*, vol. 4, no. 5, pp. 612–620, 2023. https://doi.org/10.18196/jrc.v4i5.19448
- [41] K. Singhal, V. Kumar, and K. P. S. Rana, "Robust trajectory tracking control of non-holonomic wheeled mobile robots using an adaptive fractional order parallel fuzzy PID controller," *Journal of* the Franklin Institute, vol. 359, no. 9, pp. 4160–4215, 2022. doi: https://doi.org/10.1016/j.jfranklin.2022.03.043
- [42] R. D. Puriyanto and A. K. Mustofa, "Design and implementation of fuzzy logic for obstacle avoidance in differential drive mobile robot," *Journal of Robotics and Control (JRC)*, vol. 5, no. 1, pp. 132–141, 2024. https://doi.org/10.18196/jrc.v5i1.20524
- [43] A. Baharuddin and M. Basri, "Self-tuning PID controller for quadcopter using fuzzy logic," *International Journal of Robotics and Control Systems*, vol. 3, no. 4, pp. 728–748, 2023. https://doi.org/10.31763/ijrcs.v3i4.1127
- [44] S. Louda, N. Karkar, F. Seghir et al., "Fuzzy dynamic feedback linearization for efficient mobile robot trajectory tracking and obstacle avoidance in autonomous navigation," *International Journal of Robotics and Control Systems*, vol. 5, no. 2, pp. 881– 901, 2025. https://doi.org/10.31763/ijrcs.v5i2.1780
- [45] T. P. Tho and N. T. Thinh, "Sagging cable analysis and evaluation of 4-degree-of- freedom cable robot using adaptive neural fuzzy algorithm," *International Journal of Mechanical Engineering and Robotics Research*, vol. 11, no. 2, pp. 73–78, 2022. doi: 10.18178/ijmerr.11.2.73-78
- [46] W. Faris, M. Rabie, A. Moaaz et al., "Two-flexible-link manipulator vibration reduction through fuzzy-based position," *International Journal of Robotics and Control Systems*, vol. 5, no. 1, pp. 479–499, 2025. doi: 10.31763/ijrcs.v5i1.1669
- [47] Z. Dachang, D. Baolin, Z. Puchen et al., "Constant force PID control for robotic manipulator based on fuzzy neural network algorithm," Complexity, vol. 2020, 3491845, 2020. doi: 10.1155/2020/3491845
- [48] P. Chotikunnan, B. Panomruttanarug, and P. Manoonpong, "Dual design iterative learning controller for robotic manipulator application," *Journal of Control Engineering and Applied Informatics*, vol. 24, no. 3, pp. 76–85, 2022.
- [49] P. Chotikunnan and B. Panomruttanarug, "Practical design of a time-varying iterative learning control law using fuzzy logic," *Journal of Intelligent & Fuzzy Systems*, vol. 43, no. 3, pp. 2419– 2434, 2022. doi: 10.3233/JIFS-21308
- [50] B. Panomruttanarug, R. W. Longman, and M. Q. Phan, "Steady state frequency response design of finite time iterative learning control," *The Journal of the Astronautical Sciences*, vol. 67, pp. 571–594, 2020. doi: 10.1007/s40295-019-00198-9

- [51] B. Panomruttanarug, "Position control of robotic manipulator using repetitive control based on inverse frequency response design," *International Journal of Control, Automation and Systems*, vol. 18, no. 11, pp. 2830–2841, 2020. doi: 10.1007/s12555-019-0518-2
- [52] P. Chotikunnan and R. Chotikunnan, "Dual design PID controller for robotic manipulator application," *Journal of Robotics and Control (JRC)*, vol. 4, no. 1, pp. 23–34, 2023. doi: 10.18196/jrc.v4i1.16990
- [53] S. Mahfoud, A. Derouich, N. El Ouanjli et al., "A new strategy-based PID controller optimized by genetic algorithm for DTC of the doubly fed induction motor," Systems, vol. 9, no. 2, 37, 2021. doi: 10.3390/systems9020037
- [54] C. Guo, L. Zhong, J. Zhao et al., "First order and high-order repetitive control for single - phase grid - connected inverter," *Complexity*, vol. 2020, 1094386, 2020. doi: 10.1155/2020/1094386
- [55] A. Kholiq, L. Lamidi, F. Amrinsani et al., "Development of adaptive PD control for infant incubator using fuzzy logic," *Journal* of Robotics and Control (JRC), vol. 5, no. 3, pp. 756–765, 2024. doi: 10.18196/jrc.v5i3.21510
- [56] U. Ramizares, W. Teves, E. Arboleda et al., "Intelligent temperature-controlled poultry feed dispensing system with fuzzy logic algorithm," *International Journal of Robotics and Control* Systems, vol. 4, no. 1, pp. 69–87, 2024. doi: 10.31763/ijrcs.v4i1.1256
- [57] A. O. Amole, O. E. Olabode, D. O. Akinyele et al., "Optimal temperature control scheme for milk pasteurization process using different tuning techniques for a proportional integral derivative controller," Iranian Journal of Electrical and Electronic Engineering, vol. 2170, pp. 2170–2170, 2022.
- [58] K. Anand, E. Mamatha, C. S. Reddy et al., "Design of neural network based expert system for automated lime kiln system," *Journal Européen des Systèmes Automatisés*, vol. 52, no. 4, pp. 369–376, 2019. doi: 10.18280/jesa.520406
- [59] M. Tavana and V. Hajipour, "A practical review and taxonomy of fuzzy expert systems: Methods and applications," *Benchmarking: An International Journal*, vol. 27, no. 1, pp. 81–136, 2020. doi: 10.1108/BIJ-04-2019-0178
- [60] D. Gupta and A. K. Ahlawat, "Taxonomy of GUM and usability prediction using GUM multistage fuzzy expert system," *International Arab Journal of Information Technology*, vol. 16, no. 3, pp. 357–363, 2019.

- [61] Y. A. R. Yasir, M. P. A. Posonia, and B. N. U. B. Nisha, "A graph correlated anomaly detection with fuzzy model for distributed wireless sensor networks," *International Journal of Electrical and Electronic Engineering & Telecommunications*, vol. 12, no. 5, pp. 306–316, 2023. doi: 10.18178/ijeetc.12.5.306-316
- [62] M. S. Islam and U. Chong, "Rotating machine fault detection based on fuzzy logic and improved adaptive filter," *International Journal* of Mechanical Engineering and Robotics Research, vol. 10, no. 2, pp. 79–86, 2021. doi: 10.18178/ijmerr.10.2.79-86
- [63] J. Sonawane, M. Patil, and G. K. Birajdar, "Enhancement of underwater video through adaptive fuzzy weight evaluation," *Journal of Robotics and Control (JRC)*, vol. 5, no. 2, pp. 500–508, 2024. doi: 10.18196/jrc.v5i2.20496
- [64] O. Varlamov, "Brains' for robots: Application of the Mivar expert systems for implementation of autonomous intelligent robots," Big Data Research, vol. 25, 100241, 2021. doi: 10.1016/j.bdr.2021.100241
- [65] S. Thaker and V. Nagori, "Analysis of fuzzification process in fuzzy expert system," *Procedia Computer Science*, vol. 132, pp. 1308– 1316, 2018. doi: 10.1016/j.procs.2018.05.047
- [66] K. H. D. Tang, S. Z. M. Dawal, and E. U. Olugu, "Integrating fuzzy expert system and scoring system for safety performance evaluation of offshore oil and gas platforms in Malaysia," *Journal of Loss Prevention in the Process Industries*, vol. 56, pp. 32–45, 2018. doi: 10.1016/j.jlp.2018.08.005
- [67] M. I. Fale and Y. U. G. Abdulsalam, "Dr. Flynxz-A First Aid Mamdani-Sugeno-type fuzzy expert system for differential symptoms-based diagnosis," *Journal of King Saud University-Computer and Information Sciences*, vol. 34, no. 4, pp. 1138–1149, 2022. doi: 10.1016/j.jksuci.2020.04.016
- [68] P. Chotikunnan, R. Chotikunnan, Y. Pititheeraphab et al., "Comparative analysis of fuzzy membership functions for step and smooth input tracking in a 3-axis robotic manipulator," *Journal of Fuzzy Systems and Control*, vol. 3, no. 1, pp. 39–50, 2025. doi: 10.59247/jfsc.v3i1.278

Copyright © 2025 by the authors. This is an open access article distributed under the Creative Commons Attribution License which permits unrestricted use, distribution, and reproduction in any medium, provided the original work is properly cited (CC BY 4.0).